Enhancement in mechanical quality factors of poly phenylene sulfide under high-amplitude ultrasonic vibration through thermal annealing

Jiang Wu*, Yosuke Mizuno, Kentaro Nakamura

Laboratory for Future Interdisciplinary Research of Science and Technology, Tokyo Institute of Technology, Yokohama 226-8503, Japan

ABSTRACT

Our previous study shows that poly phenylene sulfide (PPS) provides relatively high mechanical quality factors (Q factors) at ultrasonic frequency compared to other commonly-used functional polymers, and has potential as the vibrating body of a functional ultrasonic transducer. Since PPS has semicrystalline frameworks, its Q factors may be enhanced through thermal annealing. Prior to examining this feasibility, we developed a method for estimating Q factors under high-amplitude longitudinal vibration. Q factor is originally defined as the ratio of the reactive energy to the dissipated energy, both of which are calculated from the vibration velocities on the outer surface of a cylindrical specimen. Using this method, we experimentally investigated how annealing temperatures and times affect Q factors of PPS. The results demonstrate that thermal annealing is an effective way to enhance Q factors of PPS at the heating temperatures of 100 °C and 150 °C, relatively high compared to the glass transition temperature of PPS (90–95 °C). The Q factors at several tens of kilohertz are almost doubled after annealing owing to the enhancements in degrees of crystallinity. As the annealing time increases, the Q factors initially become higher, and gradually approach their saturated values at a sufficiently long time. Besides, annealing temperatures affect the change rates in Q factors, but have no observable effect on the saturated Q factors.

1. Introduction

Ultrasonic transducers are core components for high-power ultrasonic applications, e.g. ultrasonic cleaning, homogenization, atomization of liquid, and enhancement of chemical reaction [1–4]. In general, they comprise piezoelectric ceramics and vibrating bodies. Metals are commonly used as vibrating bodies in conventional ultrasonic transducers. To reduce weight of transducers, polymers are potentially applicable as vibrating bodies owing to their low densities. Moreover, it is feasible to improve production efficiencies of ultrasonic transducers as their polymer vibrating bodies can be directly fabricated by molding methods instead of machining methods [5]. We have reported that poly phenylene sulfide (PPS) exhibits low mechanical loss in high-amplitude flexural vibration [7,8], and tested several functional ultrasonic devices with PPS [5,6,8]. In particular, the PPS-based airborne ultrasonic transducers provided better performance than the commercially-available ones [8]. To gain a deeper understanding on vibrational characteristics of PPS, it would be meaningful to evaluate the mechanical loss in high-amplitude longitudinal and torsional vibrations.

Mechanical quality factors (Q factors), inversely proportional to mechanical loss, demonstrate the suitability of a material as the vibrating body [1,9]. To overcome the shortcoming of the existing methods, we proposed new methods on the basis of the original definition of Q factor, and measured the Q factors of several commonly-used polymers in flexural vibration [6], and metals in torsional vibration [10]. Since longitudinal vibration are the most widely used in industrial applications [1,4], a method is required for estimating Q factors in longitudinal vibration.

PPS belongs to semicrystalline polymers [11], of which the degree of crystallinity is thought to be increased via thermal annealing [12,13]. In general, materials with regular atomic (or molecular) frameworks, e.g. ceramics and metals, tend to exhibit low mechanical loss (high Q factors) [1]. It implies that, by carrying out thermal annealing on commercial PPS products in laboratory, their Q factors may be enhanced; however, the validity should be assessed. Besides, the relationship between Q factors and annealing conditions, e.g. temperatures and times, is required to be clarified for practical applications.

In this study, first, we introduce a new method capable of measuring Q factors in high-amplitude longitudinal vibration. To validate this method, we measure the Q factors of stainless steel, and compare the results with the previous reports. Subsequently, we estimate the strain and frequency dependences of Q factor of PPS in both longitudinal and
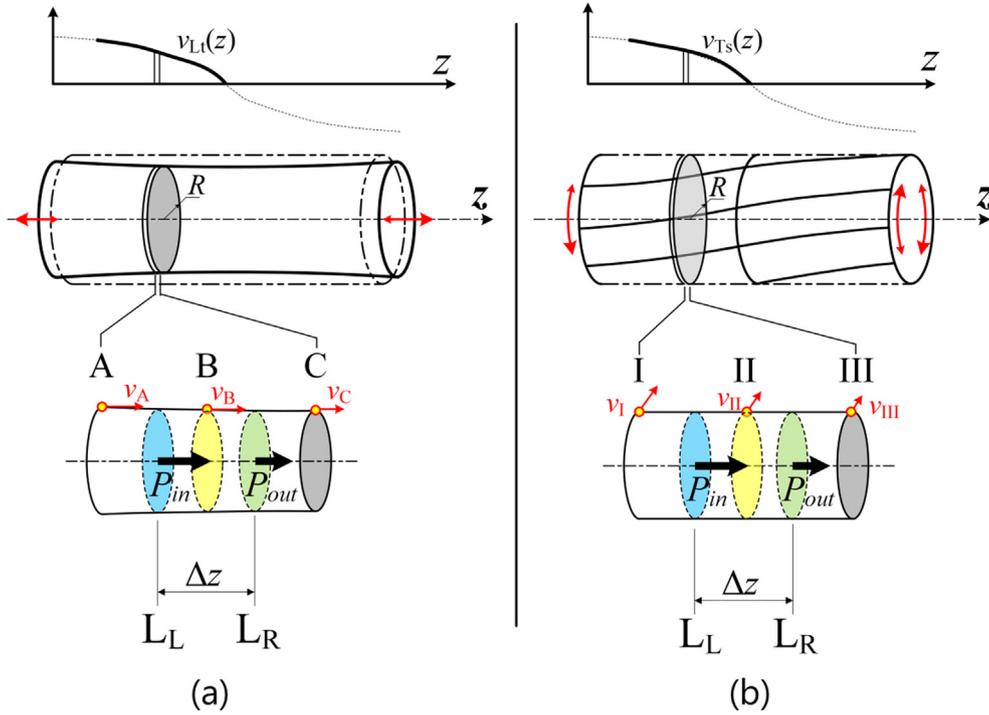

Fig. 1. Conceptual schematics of Q-factor measurements from vibration velocity distributions in (a) longitudinal and (b) torsional vibrations.

torsional vibrations. Finally, we investigate how Q factors of PPS change with varying annealing temperatures and times.

2. Principles and methods

2.1. Method for measuring Q factors in longitudinal vibration

As depicted in Fig. 1(a), longitudinal waves are excited on a cylindrical specimen. The vibration velocity distribution along the z axis $v_{Lt}(z)$ is measured on the outer surface of the specimen. The directions of the vibration velocities are parallel to the z axis. In practical measurements, the amplitudes and phases at discrete points on the surface are recorded. Points A, B, and C are adjacent sampling points with small intervals Δz. Their vibration velocities are $v_A = V_A \cdot \exp(j\theta_A)$, $v_B = V_B \cdot \exp(j\theta_B)$, and $v_C = V_C \cdot \exp(j\theta_C)$, where V_i and θ_i respectively represent the amplitude of the vibration velocity and the phase between the vibration velocity and the reference signal at the i point. The cross-sections L_L and L_R are located in the middle of points A and B, and points B and C, respectively. The local Q factor in a small region L_L–L_R equals the ratio of the reactive energy $E_{k\text{-}Lt}$ to the dissipated energy $E_{d\text{-}Lt}$ [9]:

$$Q_{Lt} = 2\pi \cdot \frac{E_{k\text{-}Lt}}{E_{d\text{-}Lt}} \bigg|_{L_L\text{-}L_R}.$$
(1)

The reactive energy $E_{k\text{-}Lt}$ stored between L_L and L_R is expressed as

$$E_{k\text{-}Lt} = \frac{1}{2}\Delta m V_B^2 = \frac{1}{2}\rho S \Delta z V_B^2,$$
(2)

where Δm denotes the mass of the region, S represents the cross-sectional area, and ρ is the density of the specimen. The mechanical constants of PPS and stainless steel, tested in this study, are listed in Table 1.

The dissipated energy $E_{d\text{-}Lt}$ is derived from the reduction in the active vibration power in a period is given as

$$E_{d\text{-}Lt} = \frac{2\pi}{\omega}(P_{in\text{-}Lt} - P_{out\text{-}Lt}),$$
(3)

where ω denotes the angular frequency, $P_{in\text{-}Lt}$ and $P_{out\text{-}Lt}$ represent the active vibration powers flowing across L_L and L_R, respectively. In longitudinal vibration, the active vibration power $P_{Lt}(z)$ across a certain cross-section is calculated from the force along the z axis $F_{Lt}(z)$ and the longitudinal vibration velocity $v_{Lt}(z)$ [14]:

$$P_{Lt}(z) = \frac{1}{2}\operatorname{Re}[F_{Lt}(z) \cdot v_{Lt}^*(z)].$$
(4)

Note that both F_{Lt} and v_{Lt} are defined as complex numbers. Re means the real part, and the asterisk indicates the complex conjugate. The relationship between $F_{Lt}(z)$ and $v_{Lt}(z)$ in longitudinal vibration is expressed as [15]

Table 1
Mechanical constants and wave speeds of PPS and stainless steel.

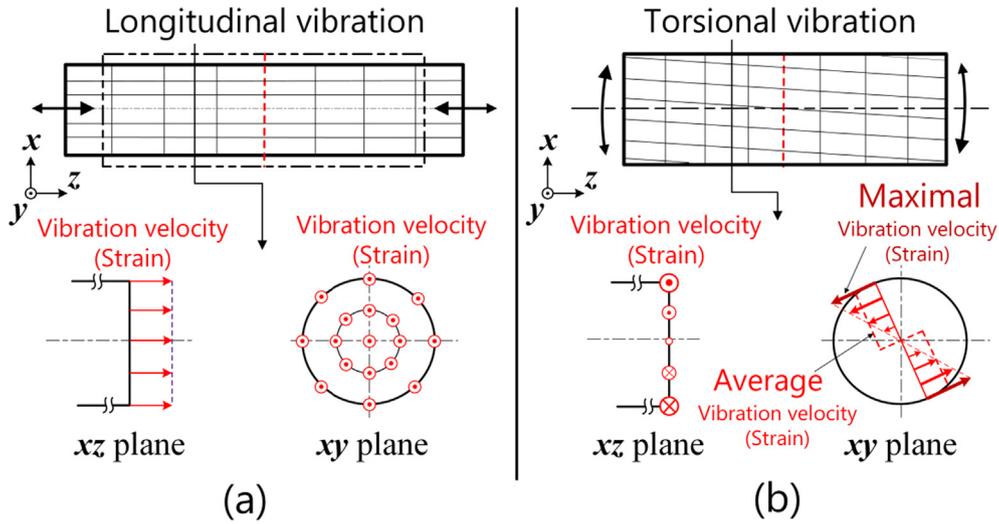| Materials	Mechanical constants			Wave speeds	
	Elastic modulus (GPa)	Density ($\times 10^3$ kg/m^3)	Poisson's ratio	Longitudinal wave speed (m/s)	Torsional wave speed (m/s)
PPS	3.45	1.35	0.36	1599	969
Stainless steel	197	7.85	0.31	5010	3095

Fig. 2. Vibration velocity (or strain) distributions on cross-sections of cylindrical specimens in (a) longitudinal and (b) torsional vibrations.

$$F_{Lt}(z) = \frac{ES}{j\omega} \cdot \frac{d[v_{Lt}(z)]}{dz},$$ (5)

where j is the imaginary unit, and E denotes the elastic modulus. Substituting Eq. (5) into (4), the active vibration power $P_{Lt}(z)$ flowing across a cross-section is given as

$$P_{Lt}(z) = -\frac{ES}{2\omega} \text{Im}\left\{ \frac{d[v_{Lt}(z)]}{dz} \cdot v_{Lt}^*(z) \right\},$$ (6)

where Im represents the imaginary part. Eq. (6) should be discretized to estimate the active power from the vibration velocities measured at two adjacent positions [15]. For example, the active power flowing into the region L_L–L_R is expressed as

$$P_{\text{in-Lt}} = -\frac{ES}{2\omega} \text{Im}\left(\frac{v_B - v_A}{\Delta z} \cdot \frac{v_A^* + v_B^*}{2} \right) = \frac{ES}{2\omega\Delta z} \cdot V_A V_B \sin(\theta_A - \theta_B).$$ (7)

Similarly, the power flowing out of the region L_L–L_R is

$$P_{\text{out-Lt}} = -\frac{ES}{2\omega} \text{Im}\left(\frac{v_C - v_B}{\Delta z} \cdot \frac{v_C^* + v_B^*}{2} \right) = \frac{ES}{2\omega\Delta z} \cdot V_B V_C \sin(\theta_B - \theta_C).$$ (8)

The strain at point B ε_B is given as

$$\varepsilon_B = \frac{1}{2}(\varepsilon_B^- + \varepsilon_B^+) = \frac{1}{2\omega j} \cdot \left(\frac{v_B - v_A}{\Delta z} + \frac{v_C - v_B}{\Delta z} \right),$$ (9)

where ε_B^- and ε_B^+ are the strains in the regions A–B and B–C, respectively. In theory, from the vibration velocities of three adjacent
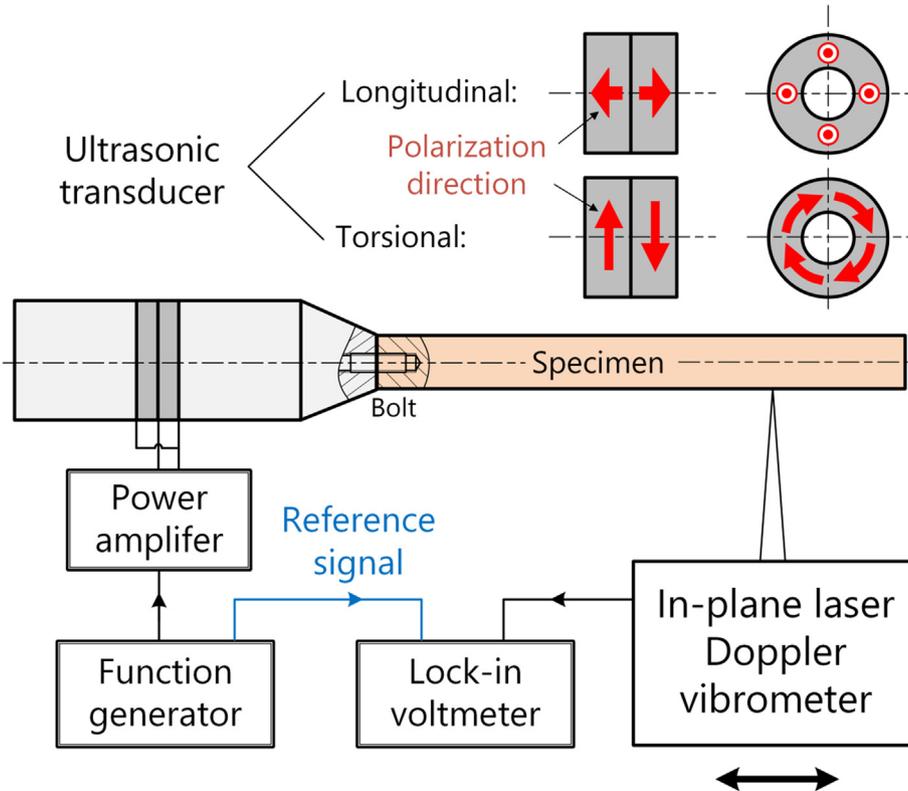

Fig. 3. Schematic of experimental setup. Using the transducers with piezoelectric ceramic elements polarized along the horizontal and circumferential directions, longitudinal and torsional vibrations can be excited on the specimens, respectively.

points, the local Q factor and strain in the small region L_L–L_R are obtained. If the vibration velocities are measured over a large length along the z axis, it is capable of estimating the strain dependence of Q factor as the wave amplitudes decay gradually along the propagating direction.

2.2. Method for measuring Q factors in torsional vibration

Ref. [10] has reported the Q-factor measurement method in torsional vibration. Here, we briefly introduce this method as it is heavily used in the study. It has two differences compared to the aforementioned method in longitudinal vibration. First, in torsional vibration, the vibration velocities are measured orthogonally to the z axis [(see Fig. 1(b)]. Second, as depicted in Fig. 2(a), the vibration velocities are uniformly distributed on a cross-section in longitudinal vibration. Whereas, Fig. 2(b) demonstrates that, in torsional vibration, the vibration velocity on a cross-section decreases linearly from the outer surface to the central axis [16,17]. As Fig. 1(b) shows, when the vibration velocities at three adjacent points I, II, and III are respectively $v_I = V_I \cdot \exp(j\theta_I)$, $v_{II} = V_{II} \cdot \exp(j\theta_{II})$, and $v_{III} = V_{III} \cdot \exp(j\theta_{III})$, the reactive energy $E_{k\text{-Ts}}$, the input active power $P_{\text{in-Ts}}$, and the output active power $P_{\text{out-Ts}}$ can be calculated using the equations

$$E_{k\text{-Ts}} = \frac{1}{2}\rho \cdot \Delta z \cdot \int_0^R \left(V_{II} \cdot \frac{r}{R}\right)^2 \cdot 2\pi r dr = \frac{\pi}{4}\rho R^2 V_{II}^2 \Delta z, \tag{10}$$

$$P_{\text{in-Ts}} = -\text{Im}\left\{\frac{G}{\omega}\int_0^R \left(\frac{r}{R}\right)^2 \frac{d[v_{Ts}(z)]}{dz}v_{Ts}^*(z)\cdot 2\pi r dr\right\}\Bigg|_{z=L_L}$$
$$= \frac{G\pi R^2}{2\omega\Delta z}\cdot V_I V_{II}\sin(\theta_I - \theta_{II}), \tag{11}$$

and

$$P_{\text{out-Ts}} = \frac{G\pi R^2}{2\omega\Delta z}\cdot V_{II} V_{III}\sin(\theta_{II} - \theta_{III}), \tag{12}$$

respectively, where G denotes the shear modulus, and R represents the radius of the specimen. The strain distributions on cross-sections are completely the same to the vibration velocity distributions. It is worth pointing out that, in torsional vibration, the result derived from the vibration velocities measured on the outer surface with Eq. (9) are the maximal strain; half of this value reflects the average strain on a cross-section.

3. Experimental results

3.1. Experimental setup

To verify whether the mechanical loss can be correctly evaluated by our method, we measured the Q factors of a stainless steel cylindrical bar in longitudinal vibration, and compared the results with the previously-reported values [18]. The experimental setup is schematically shown in Fig. 3. Longitudinal transducers with different frequencies
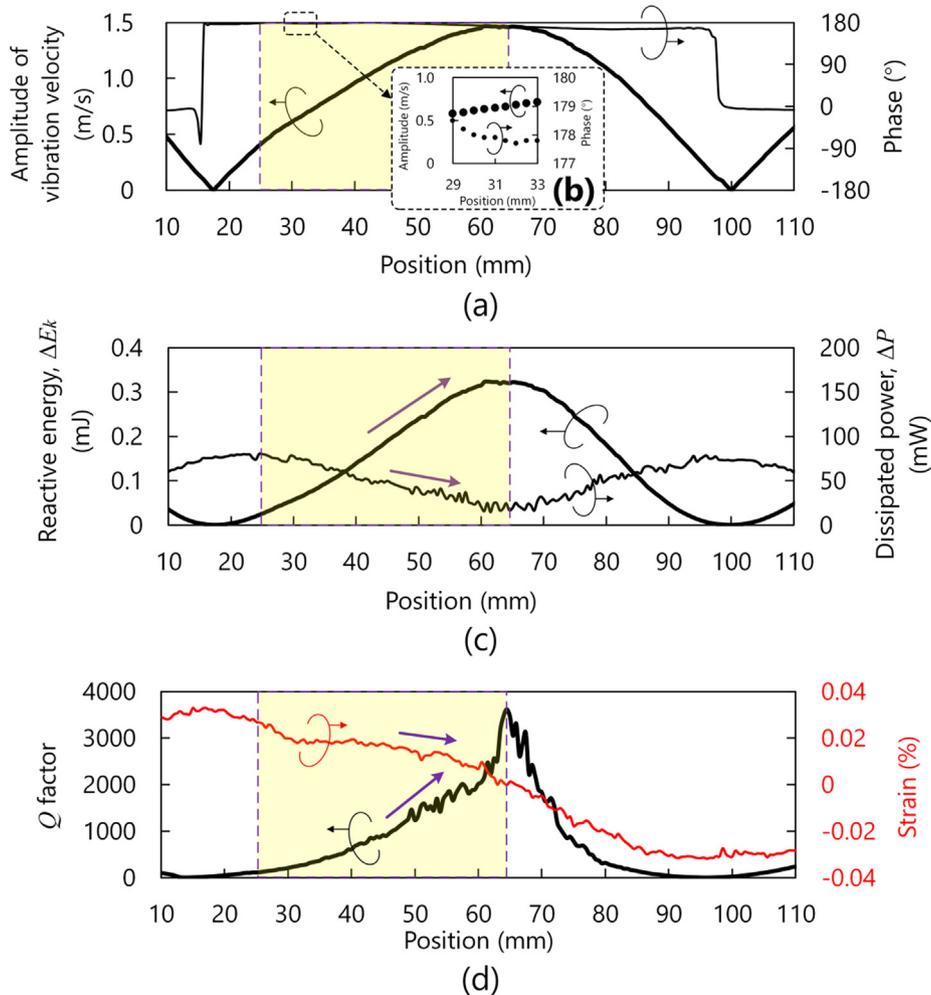

Fig. 4. Distributions of vibration velocity in the z ranges of (a) 10–110 mm and (b) 29–34 mm, (c) reactive energy and dissipated power, and (d) local Q factor and strain in the z range of 10–110 mm.
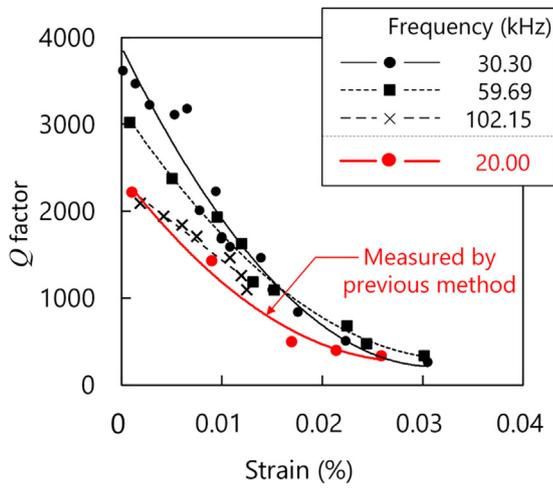
Fig. 5. Q factor of stainless steel as a function of strain under different frequencies.

were employed to excite ultrasonic vibration on a 10-mm-diameter 500-mm-long stainless steel specimen, of which one end was connected to the transducers with bolts. When voltages were applied, longitudinal vibration was generated on the specimens. An in-plane laser Doppler vibrometer (IPV100, Polytec, Waldbronn, Germany) mounted on a guide rail was moved along the z axis. The vibration velocities in the z range from 10 to 110 mm were measured with an interval of 0.5 mm. The amplitudes of the vibration velocities and the phases between the vibration velocities and the reference signal were detected with a lock-in voltmeter (5560, NF Electronic Instruments, Yokohama, Japan).

3.2. Q factors of stainless steel

When a sinusoidal voltage with an amplitude of 30 V and a frequency of 30.30 kHz were applied, as shown in Fig. 4(a), a standing wave with a maximal vibration velocity of approximately 1.5 m/s was excited on the stainless steel specimen. Note that the driving frequency was set to the resonance frequency of the entire vibration system composed of both the transducer and specimen. Half of the wavelength and the driving frequency are 82 mm and 30.30 kHz, respectively.
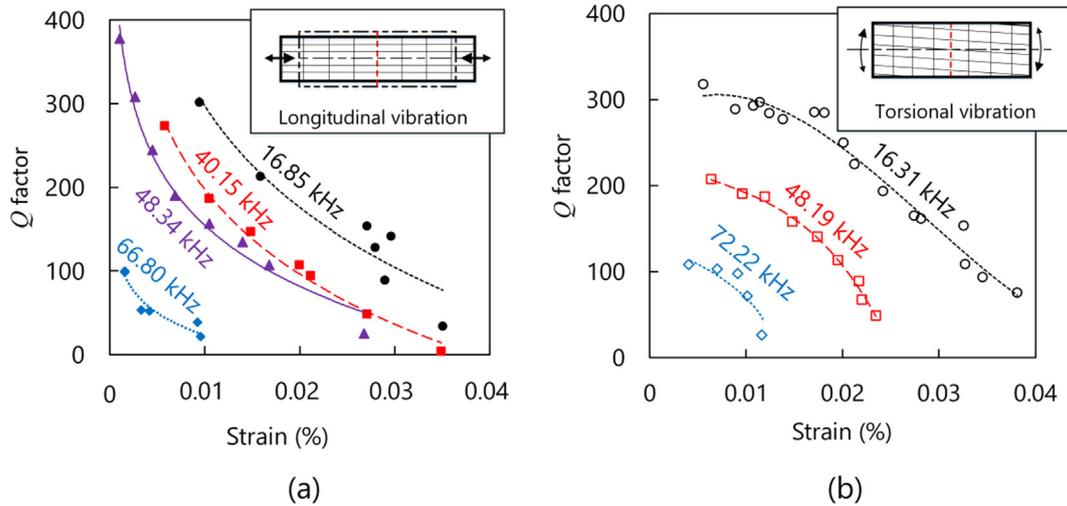

Fig. 6. Q factors of PPS as functions of strain under different frequencies in (a) longitudinal and (b) torsional vibrations.
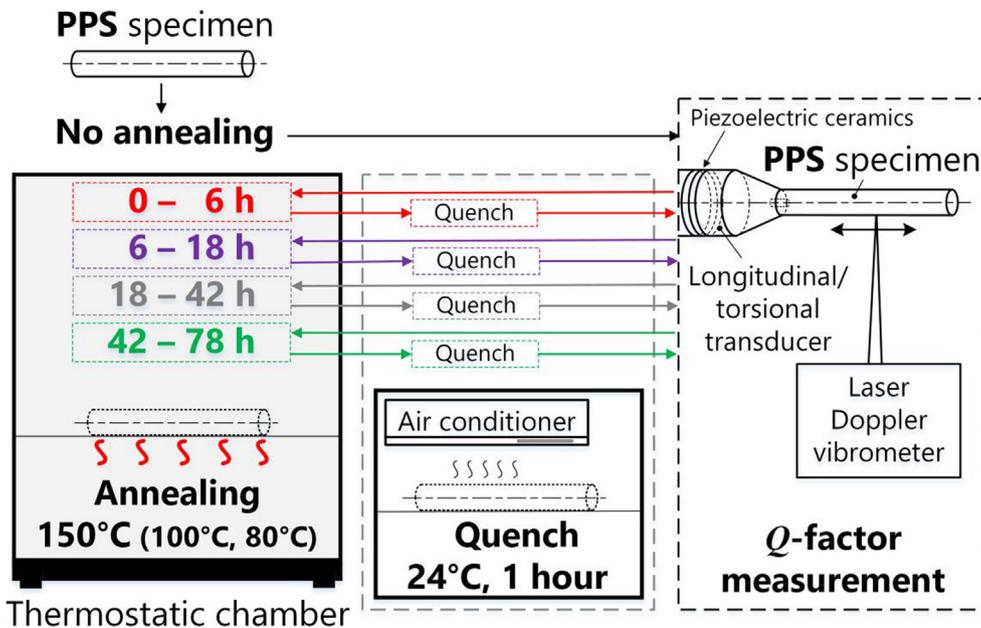

Fig. 7. Experimental procedures for investigating the effects of annealing temperatures and times on Q factors of PPS.

Therefore, the wave speed is estimated to be 4969 m/s, close to the theoretical longitudinal speed in stainless steel (see Table 1). It infers that the longitudinal vibration was successfully generated on the specimen. Fig. 4(b) illustrates that there exist small variations in phases. Though they are not observable in the overall phase distribution, the variations enable nonzero values of the calculated local active powers. Fig. 4(c) illustrates that, as *z* ranges from 25 to 64 mm, the reactive energy monotonically increased from 0.03 to 0.32 mJ. In contrast, the dissipated power yielded a reduction from 80 to < 15 mW. It can be observed from Fig. 4(d) that the *Q* factor becomes higher with reducing strain, though there exist several fluctuations, which are possibly caused by measurement errors in vibration velocities. Fig. 5 shows the measured strain dependences of *Q* factor of stainless steel at different frequencies. At 30.30 kHz, the *Q* factor reached approximately 3600 at the strain of lower than 0.002%, and sharply decreased to 260 when the strain was reduced to 0.03%. At 0.005% strain, the *Q* factor exceeded 3000 at 30.30 kHz, and decreased to 2000 when the driving frequency increased to 102.15 kHz.

Ref. [18] has introduced a method for measuring strain dependence of *Q* factors: A magnetostrictive transducer was employed to excite longitudinal vibration on a stainless steel specimen. The mechanical losses were measured before and after the specimen was fixed to the transducer, and the *Q* factors were derived from their difference. By adjusting the voltage applied to the transducer, how *Q* factors depend on strains was investigated. For comparison, the results are plotted in Fig. 5. Observably, our *Q* factors measured by our method have the same tendencies with the previous results. However, at the strain of < 0.005%, our *Q* factors are higher than the values given in Ref. [18] because the mechanical loss generated on the contacting surface between the sample and the exciter (stainless steel bar and piezoelectric transducer, respectively, in this study) is excluded [6].

3.3. Strain and frequency dependences of Q factor of PPS

The 10-mm-diameter 250-mm-long PPS specimens used in this study are TORAY's products. Fig. 6(a) and (b) demonstrate the strain dependences of *Q* factor of the PPS specimen under longitudinal and torsional vibrations, respectively. Note that the abscissa of Fig. 6(b) represents the average strain. In longitudinal vibration, the *Q* factor at 48.34 kHz exceeded 300 when the strain was lower than 0.003%, and decreased to approximately 100 when the strain increased to 0.018%. When the strain was 0.01%, the *Q* factor decreased from 300 to 20 as
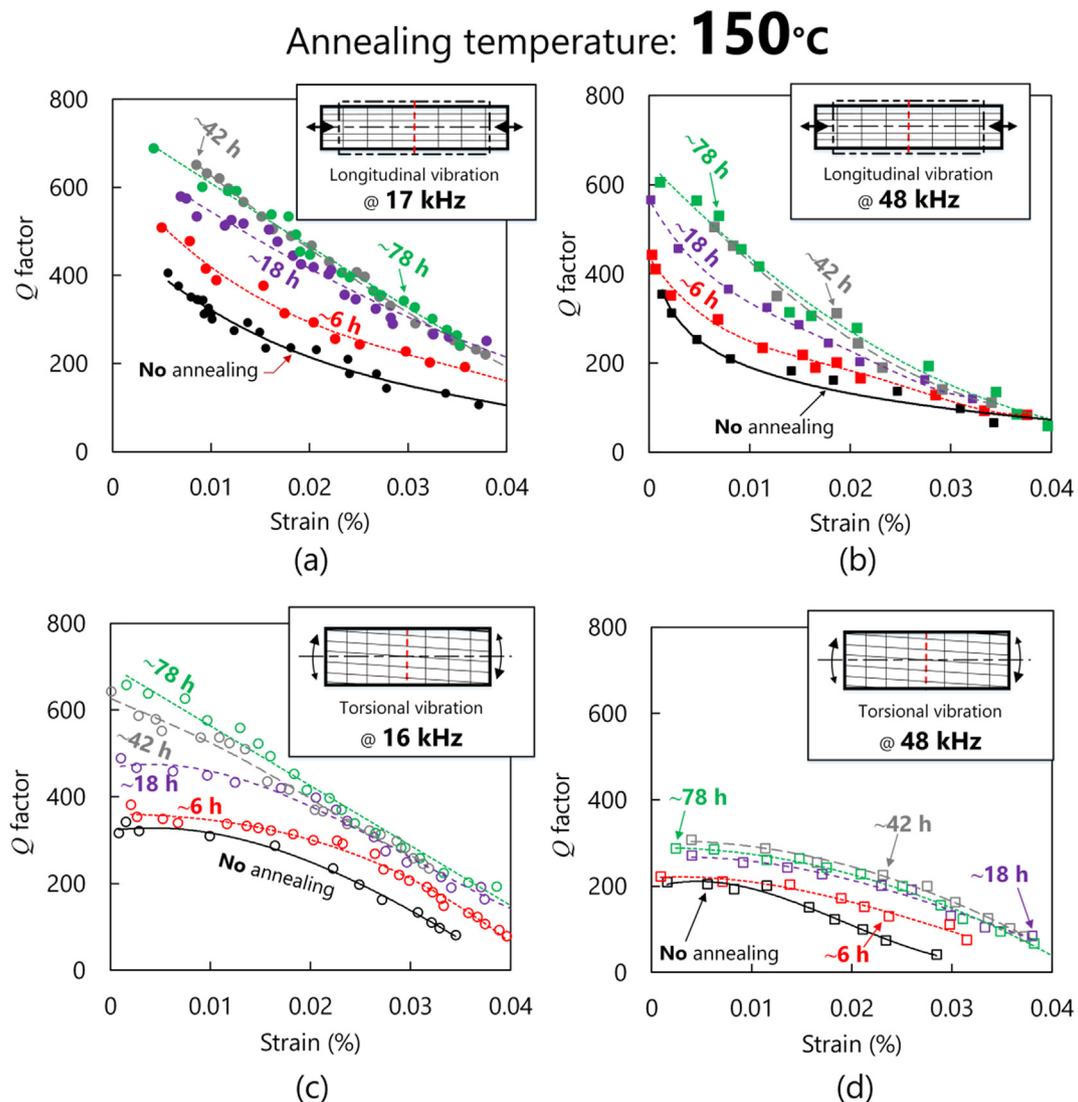

Fig. 8. Strain dependences of *Q* factor of PPS with varying annealing time. The annealing temperature is 150 °C. (a) and (b) Show the *Q* factors in longitudinal vibrations with frequencies of 17 and 48 kHz, respectively. (c) and (d) Are the *Q* factors in torsional vibrations with frequencies of 16 and 48 kHz, respectively.
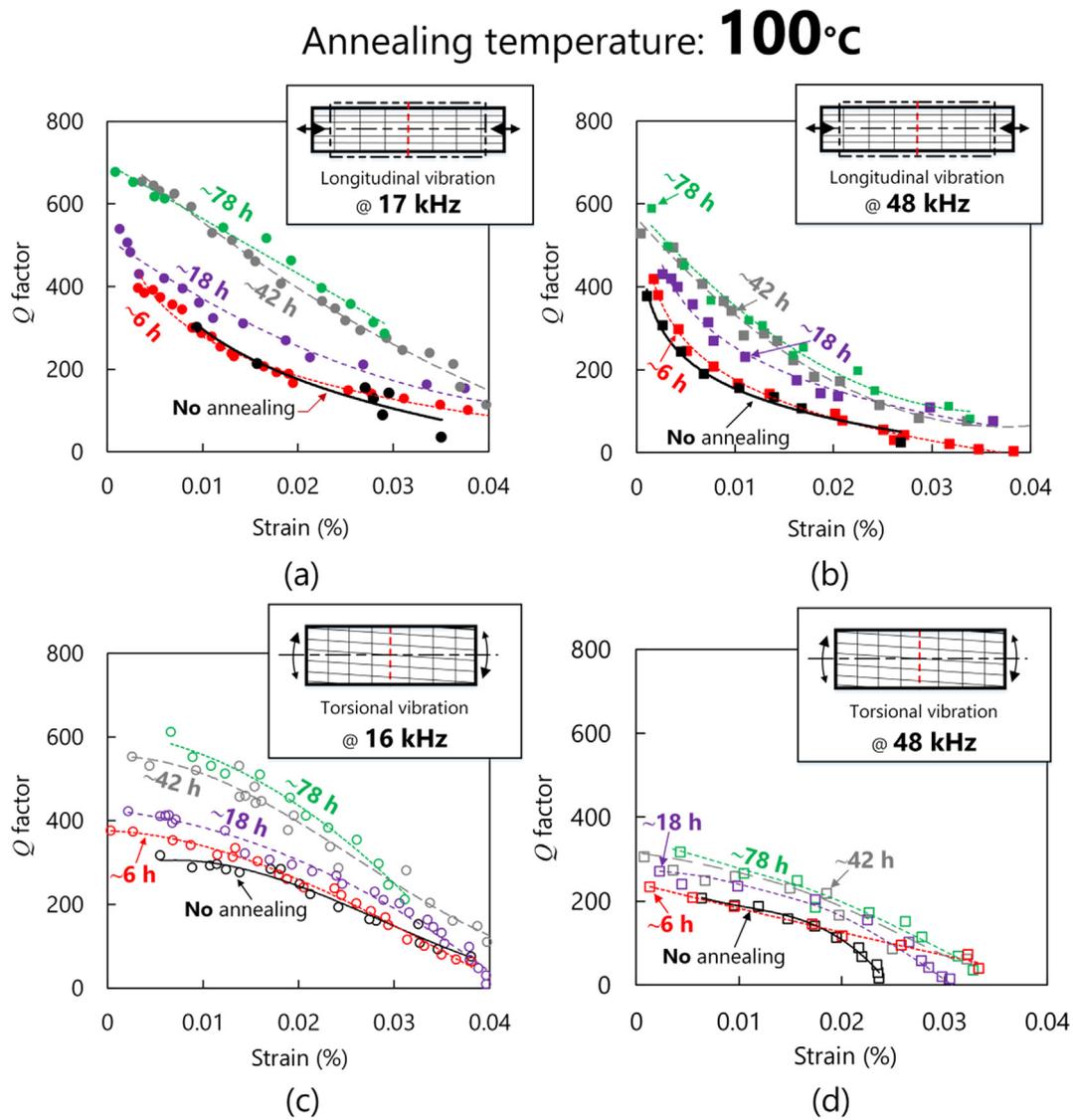
Fig. 9. Strain dependences of Q factor of PPS with varying annealing time. The annealing temperature is 100 °C. (a), (b); (c) and (d) are the Q factors measured at 17 and 48 kHz in torsional vibrations; and at 16 and 48 kHz in torsional vibrations, respectively.

the frequency increased from 16.85 to 66.80 kHz. In Fig. 6(b), at 16.31 kHz and < 0.005% strain, the Q factors exceeded 300. Clearly, as the strain and the frequency become higher, there are observable decreases in the Q factors of PPS in both longitudinal and torsional vibrations. In particular, when the strains were lower than 0.01%, the Q factors in longitudinal vibration have sharp reductions, but they are still higher than the values in torsional vibration. Similar tendencies can also be found in the cases of stainless steel specimens [10,18]. It is assumed to originate from the non-uniformity of the mechanical loss along the radial direction in torsional vibration. As mentioned above, the strain near the outer surface is theoretically twice the average strain on a cross-section. Since the strains greatly affect the mechanical loss particularly at low strains [1], the mechanical loss near the outer surface should be higher than the average mechanical loss on the cross-section (the Q factors near the outer surface is lower the average Q factors). In contrast, as the mechanical loss in longitudinal vibration is uniformly distributed on a cross-section, the Q factors at the surfaces should have negligible differences with the average Q factors. Thus, at a certain strain of < 0.01%, the Q factors are lower for torsional vibration than for longitudinal vibration.

4. Effects of annealing temperature and time on Q factors of PPS

After clarifying how strain and frequency affect Q factors of PPS, in this section, we explore the how Q factors change with varying annealing conditions. Fig. 7 illustrates the experimental procedures:

(1) Measure the Q factors of the PPS specimen without annealing.
(2) Anneal the specimen for 6 h in a thermostatic chamber, of which the temperature was maintained at 150 °C.
(3) Quench at 24 °C in air for 1 h.
(4) Measure the vibration velocities in the same region, and calculate the Q factors. Cut a 2-mm-thick part from the free end of the PPS specimen for measuring the degree of crystallinity.

Following the procedures (2)–(4), the Q factors were measured when the annealing time reaches 18, 42, and 78 h. Another two PPS specimens were heated at 100 °C and 80 °C, and the same measurements were performed. To obtain observable variations in Q factors, we gradually increase the annealing intervals between measurements (6h → 12 h → 24 h → 36 h), though they are generally set to constants in

Annealing temperature: **80°C**
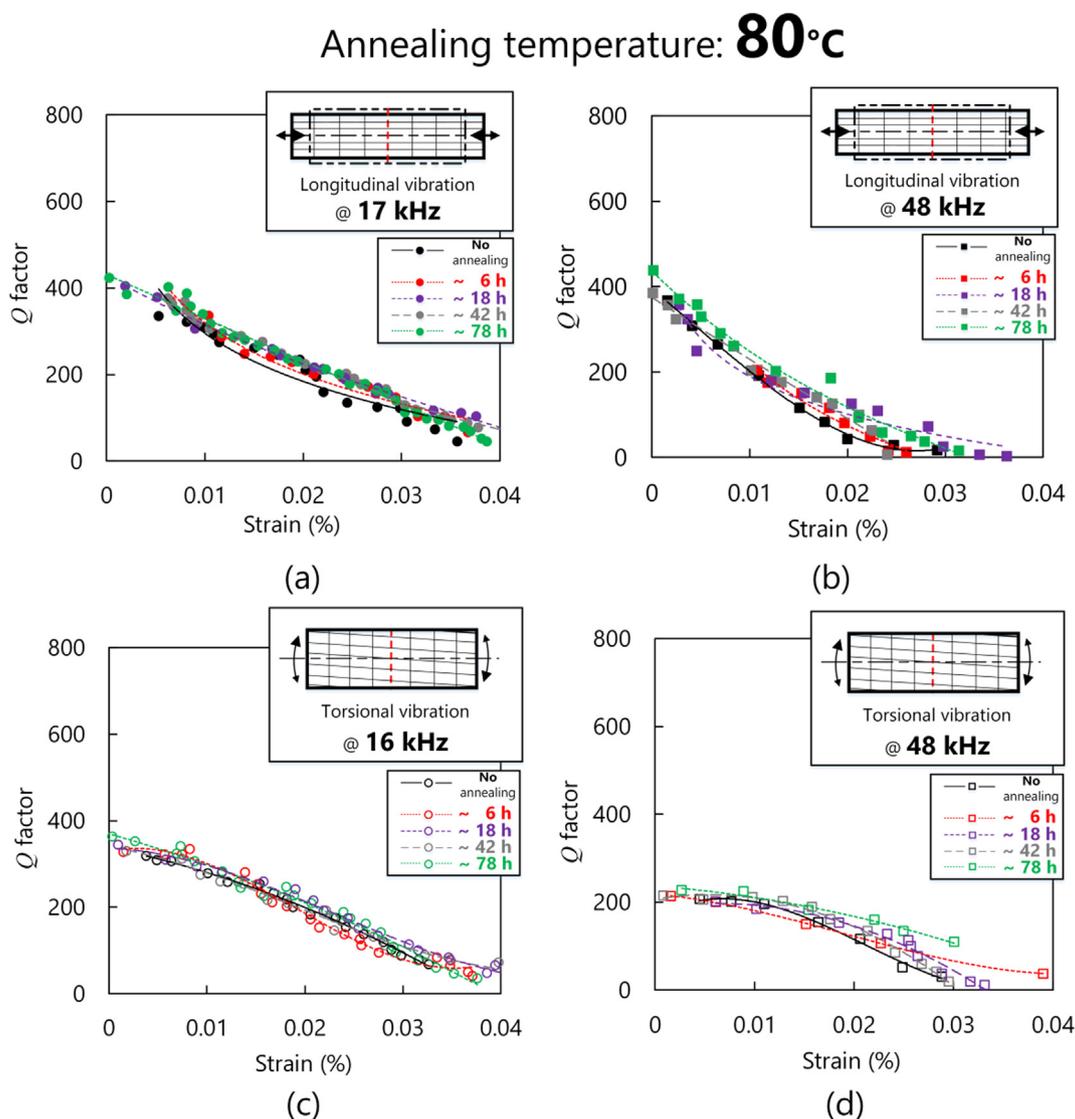
Fig. 10. Strain dependences of Q factor of PPS with varying annealing time. The annealing temperature is 80 °C. (a), (b); (c), and (d) are the Q factors in longitudinal vibrations with frequencies of 17 and 48 kHz; and in torsional vibrations with frequencies of 16 and 48 kHz, respectively.

previous studies [11,19]. Besides, it has been reported that the elastic moduli and densities of semicrystalline polymers become higher after annealing owing to the increase in degrees of crystallinity [1,14]. However, after PPS was annealed at 155 °C for 48 h, its elastic modulus and density increased by < 0.16 GPa and < 0.10 × 10³ kg/m³, respectively [20,21]; such small variations should cause negligible measurement errors. Thus, we did not change the mechanical constants when calculating the Q factors under different annealing conditions.

Fig. 8(a) and (b) show the Q factors in longitudinal vibration when the driving frequencies are approximately 17 and 48 kHz, respectively. When the frequency was 17 kHz and the strain was 0.01%, the Q factor was 300 before annealing, and became higher with increasing time, and leveled off when the PPS specimen was annealed for 42 h. At 48 kHz and 0.01% strain, the Q factor reached 436 after annealing for 78 h. Fig. 8(c) and (d) demonstrate that, in torsional vibration, the Q factors also exhibit observable enhancements via annealing. At 16 kHz, the saturated Q factor exceeded 600, close to the value in longitudinal vibration with approximately the same frequency (17 kHz). However, at

48 kHz, the saturated Q factor in torsional vibration was approximately 310, relatively low compared to the value in longitudinal vibration.

Fig. 9 plots the Q factors of PPS annealed at 100 °C. Before annealing, the strain dependences of Q factor of this PPS specimen (the black dots in Fig. 9) have unobservable differences with those of the former specimen (the black dots in Fig. 8). In Fig. 9(a), at 17 kHz and 0.01% strain, the Q factors increased by 60 after annealing for 18 h. When the annealing temperature was maintained at 150 °C, the Q factors increased by 213 after the PPS specimen was annealed for 18 h. The saturated Q factor, obtained after annealing for 78 h, reached 602, close to 621, the value obtained at 150 °C. Clearly, annealing temperatures affect the change rates in Q factors ($\Delta Q/\Delta t$), but have little influence on the saturated Q factors. The results in Fig. 9(b)–(d) also support this conclusion.

Fig. 10 shows the Q factors of PPS at the heating temperature of 80 °C. The Q factors exhibit unobservable variations though the PPS specimen was annealed for 78 h; this time is sufficiently long for achieving considerable Q-factor changes at 100 °C and 150 °C. To
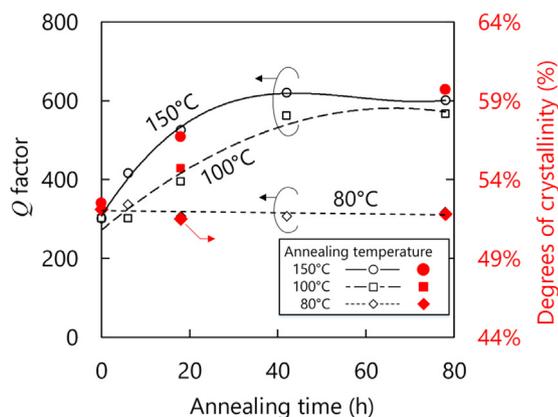
Fig. 11. *Q* factors of PPS in longitudinal vibration at 17 kHz and 0.01% strain and degrees of crystallinity as functions of annealing time under different temperatures.

explain the reason for the *Q*-factor variations, the degrees of crystallinity of PPS samples with different annealing temperatures and times were analyzed by the X-ray diffraction method [22,23] [this analysis was carried out by our agent company with a diffractometer (D2 PHASER, Bruker, Billerica, USA)]. The results as well as the *Q* factors in longitudinal vibration at 17 kHz and 0.01% strain are illustrated in Fig. 11. Clearly, the *Q* factors have identical tendencies with the degrees of crystallinity. It indicates that the *Q*-factor enhancements of PPS annealed at 100 °C and 150 °C are caused by the increases in the degrees of crystallinity. However, there are almost no changes in the degrees of crystallinity, and consequently in the *Q* factors at the heating temperature of 80 °C probably because it is below the glass-transition temperature of PPS (90–95 °C) [24].

5. Conclusions

Using our developed *Q*-factor measurement method, first, we clarified the strain and frequency dependences of *Q* factors of PPS, and subsequently investigated how annealing temperature and time affect the *Q* factors. Through our experiments, we have drawn the following conclusions:

(1) A method for measuring strain and frequency dependences of *Q* factor in high-amplitude longitudinal vibration is developed.
(2) The *Q* factors of PPS become lower with increasing strain and frequency in both longitudinal and torsional vibrations.
(3) It is capable of increasing *Q* factors of PPS via thermal annealing at 100 °C and 150 °C; these heating temperatures are higher than the glass-transition temperature of PPS.
(4) The enhancements in *Q* factors of PPS originate from the increases in degrees of crystallinity after thermal annealing.
(5) The change rates in the *Q* factors is affected by annealing temperatures. However, the saturated *Q* factors are independent of annealing temperatures.

This study demonstrates the effectiveness of *Q*-factor enhancement of PPS through thermal annealing. The explorations of optimal annealing conditions, such as temperatures, times, and atmospheres of annealing as well as quenching, would provide a meaningful knowledge towards the practical applications of PPS to functional ultrasonic devices. It is also worth investigating whether thermal annealing is capable of improving the *Q* factors of other low-mechanical-loss polymers, e.g. poly ether ether ketone (PEEK) [5,6], in further studies.

References

[1] K. Takagi, et al., Ultrasonic Handbook, Maruzen Publication, Tokyo, Japan, 1999 (In Japanese).
[2] T.J. Mason, Industrial sonochemistry: potential and practicality, Ultrasonics 30 (1992) 192–196.
[3] T.J. Mason, Sonochemistry and sonoprocessing: the link, the trends, and (probably) the future, Ultrason. Sonochem. 10 (2003) 175–179.
[4] S. Sato, Y. Wada, D. Koyama, K. Nakamura, Estimation of absolute sound press in a small-sized sonochemical reactor, Ultrason. Sonochem. 20 (2003) 468–471.
[5] J. Wu, Y. Mizuno, M. Tabaru, K. Nakamura, Ultrasonic motors with polymer-based vibrators, IEEE Trans. Ultrason. Ferroelectr. Freq. Control 62 (2015) 2169–2178.
[6] J. Wu, Y. Mizuno, M. Tabaru, K. Nakamura, Measurement of mechanical quality factors of polymers in flexural vibration for high-power ultrasonic application, Ultrasonics 69 (2016) 74–82.
[7] J. Wu, Y. Mizuno, K. Nakamura, Polymer-based ultrasonic motors utilizing high-order vibration modes, IEEE/ASME Trans. Mechatron. 23 (2018) 788–799.
[8] J. Wu, Y. Mizuno, M. Tabaru, K. Nakamura, Airborne ultrasonic transducer using polymer-based elastomer with high output-to-weight ratio, Jpn. J. Appl. Phy. 54 (2015) 087201.
[9] B.F. Ley, S.G. Lutz, C.F. Rehberg, Linear Circuit Analysis, McGraw-Hill Inc., New York, NY, USA, 1959.
[10] K. Nakamura, K. Kakihara, M. Kawakami, S. Ueha, Measuring vibration characteristics at large amplitude region of materials for high power ultrasonic vibration system, Ultrasonics 38 (2000) 122–126.
[11] J.P. Jog, V.M. Nadkarni, Crystallization kinetics of polyphenylene sulfide, J. Appl. Polym. Sci. 30 (1995) 997–1009.
[12] L.C.E. Struik, The mechanical and physical ageing of semicrystalline polymers: 1, Polymer 28 (1987) 1521–1533.
[13] A. Lukashov, V. Feofanov, J.D. Schultze, M. Boehning, J. Springer, Acoustic properties of poly phenylene sulphide, Polymer 33 (1992) 2227–2228.
[14] S. Ueha, M. Kuribayashi, Y. Tsuda, E. Mori, Y. Hashimoto, An ultrasonic power meter, J. Acoust. Soc. Am. 79 (1986) 985–989.
[15] R. Morikawa, S. Ueha, K. Nakamura, Error evaluation of the structural intensity measured with a scanning laser Doppler vibrometer and a *k*-space signal processing, J. Acoust. Soc. Am. 99 (1996) 2913–11921.
[16] S.P. Timoshenko, Strength of Materials: Part I Elementary, third ed., Van Nostrand Reinhold Company, New York, 1955.
[17] S.P. Timoshenko, D.H. Young, W. Weaver, Vibration Problems in Engineering, fourth ed., John Wiley & Sons, New York, 1974.
[18] A. Sugiyama, et al., Ultrasonic Industry, Tokyo, Corona Publ, Japan, 1993 (In Japanese).
[19] Y. Liu, T. Maeda, Y. Yokouchi, T. Morita, The hardening of CuO–(K, Na)NbO3 via post annealing with argon, Jpn. J. Appl. Phys. 53 (2014) 015503.
[20] T. Nishino, K. Tada, K. Nakamae, Elastic modulus of crystalline regions of poly (ether ether ketone), poly (ether ketone), and poly (p-phenylene sulphide), Polymer 33 (1992) 736–743.
[21] M. Bonnet, K.-D. Rogausch, J. Petermann, The endothermic "annealing peak" of poly (phenylene sulphide) and poly (ethylene terephthalate), Colloid. Polym. Sci. 277 (1999) 513–518.
[22] H.P. Klug, L.E. Alexander, X-ray Diffraction Procedures for Polycrystalline and Amorphous Materials, second ed., Wiley, New York, USA, 1974.
[23] N.S. Murthy, H. Minor, General procedure for evaluating amorphous scattering and crystallinity from X-ray diffraction scans of semicrystalline polymers, Polymer 31 (1990) 996–1002.
[24] Thermal properties of TOREY's PPS product: TORELINA, < http://www.toray.jp/plastics/en/torelina/technical/tec_013.html > .

Jiang Wu was born in Liaoning, China, on January 29, 1988. He received the B.E. degree in mechanical engineering from Dalian University of Technology, China, in 2010. From 2010 to 2012, he studied in the State Key Laboratory of Robotics and System, Harbin Institute of Technology (HIT), China, and received the M.E. degree in mechatronic engineering from HIT in 2012. From 2012 to 2017, he studied in the Future Interdisciplinary Research of Science and Technology, Tokyo Institute of Technology (TITECH), Japan, and received Dr. Eng. degree in electrical and electronic engineering from TITECH in 2017. His research interest includes piezoresistive and piezoelectric materials, permanent-magnet-based sensing technology, and polymer-based ultrasonic transducers and actuators.

Yosuke Mizuno (M'14–SM'17) was born in Hyogo, Japan, on October 13, 1982. He received the B.E., M.E., and Dr. Eng. degrees in electronic engineering from the University of Tokyo, Japan, in 2005, 2007, and 2010, respectively.

From 2007 to 2010, he was involved in Brillouin optical correlation-domain reflectometry for his Dr. Eng. degree at the University of Tokyo. From 2007 to 2010, he was a Research Fellow (DC1) of the Japan Society for the Promotion of Science (JSPS). From 2010 to 2012, as a Research Fellow (PD) of JSPS, he worked on polymer optics at Tokyo Institute of Technology, Japan. Since 2012, he has been an Assistant Professor at the Precision and Intelligence Laboratory (presently, Institute of Innovative Research), Tokyo Institute of Technology, where he is active in fiber-optic sensing, polymer optics, and ultrasonics.

Dr. Mizuno is the winner of the Ando Incentive Prize for the Study of Electronics in 2011, the Tokyo Tech Challenging Research Award in 2013, the Konica Minolta Imaging Science Award in 2014, and the Japanese Society of Applied Physics (JSAP) Young Scientist Presentation Award in 2015. He is a member of the IEEE Photonics Society (Senior Member), the JSAP, and the Institute of Electronics, Information, and Communication Engineers of Japan.

Kentaro Nakamura (M'00) was born in Tokyo, Japan, on July 3, 1963. He received the B.E., M.E., and Dr. Eng. degrees from Tokyo Institute of Technology, Japan, in 1987, 1989, and 1992, respectively.

Since 2010, he has been a Professor at the Precision and Intelligence Laboratory (presently, Institute of Innovative Research), Tokyo Institute of Technology. His research field is the applications of ultrasonic waves, measurement of vibration and sound using optical methods, and fiber-optic sensing.

Prof. Nakamura is the winner of the Awaya Kiyoshi Award for Encouragement of Research from the Acoustical Society of Japan (ASJ) in 1996, and the Best Paper Awards from the Institute of Electronics, Information and Communication Engineers (IEICE) of Japan in 1998 and from the Symposium on Ultrasonic Electronics in 2007 and 2011. He also received the Japanese Journal of Applied Physics Editorial Contribution Award from the Japan Society of Applied Physics (JSAP) in 2007. He is a member of the IEEE, the ASJ, the JSAP, the IEICE, and the Institute of Electrical Engineers of Japan.